In vivo and ex vivo epi-mode pump-probe imaging of melanin and microvasculature

Thomas E. Matthews,[1] Jesse W. Wilson,[1] Simone Degan,[1] Mary Jane Simpson,[1] Jane Y. Jin,[2] Jennifer Y. Zhang,[2] and Warren S. Warren[1,3,*]

[1]Department of Chemistry, Duke University, Durham, NC 27708, USA
[2]Department of Dermatology, Duke University School of Medicine, Durham, NC 27710, USA
[3]Department of Radiology, Duke University Medical Center, Durham, NC 27710, USA
**warren.warren@duke.edu*

Abstract: We performed epi-mode pump-probe imaging of melanin in excised human pigmented lesions and both hemoglobin and melanin in live xenograft mouse melanoma models to depths greater than 100 μm. Eumelanin and pheomelanin images, which have been previously demonstrated to differentiate melanoma from benign lesions, were acquired at the dermal-epidermal junction with cellular resolution and modest optical powers (down to 15 mW). We imaged dermal microvasculature with the same wavelengths, allowing simultaneous acquisition of melanin, hemoglobin and multiphoton autofluorescence images. Molecular pump-probe imaging of melanocytes, skin structure and microvessels allows comprehensive, non-invasive characterization of pigmented lesions.

OCIS codes: (170.3880) Medical and biological imaging; (180.5810) Scanning microscopy; (320.7150) Ultrafast spectroscopy.

References and links

1. B. G. Wang, K. König, and K. J. Halbhuber, "Two-photon microscopy of deep intravital tissues and its merits in clinical research," J. Microsc. **238**(1), 1–20 (2010).
2. T. H. Tsai, S. H. Jee, C. Y. Dong, and S. J. Lin, "Multiphoton microscopy in dermatological imaging," J. Dermatol. Sci. **56**(1), 1–8 (2009).
3. L. V. Wang, "Multiscale photoacoustic microscopy and computed tomography," Nat. Photonics **3**(9), 503–509 (2009).
4. C. Krafft, G. Steiner, C. Beleites, and R. Salzer, "Disease recognition by infrared and Raman spectroscopy," J Biophotonics **2**(1-2), 13–28 (2009).
5. C. L. Evans and X. S. Xie, "Coherent anti-stokes Raman scattering microscopy: chemical imaging for biology and medicine," Annu Rev Anal Chem (Palo Alto Calif) **1**(1), 883–909 (2008).
6. A. Scope, C. Benvenuto-Andrade, A. L. C. Agero, J. Malvehy, S. Puig, M. Rajadhyaksha, K. J. Busam, D. E. Marra, A. Torres, I. Propperova, R. G. Langley, A. A. Marghoob, G. A. Pellacani, S. Seidenari, A. C. Halpern, and S. Gonzalez, "In vivo reflectance confocal microscopy imaging of melanocytic skin lesions: consensus terminology glossary and illustrative images," J. Am. Acad. Dermatol. **57**(4), 644–658 (2007).
7. M. Rajadhyaksha, M. Grossman, D. Esterowitz, R. H. Webb, and R. R. Anderson, "*In vivo* confocal scanning laser microscopy of human skin: melanin provides strong contrast," J. Invest. Dermatol. **104**(6), 946–952 (1995).
8. J. T. Oh, M. L. Li, H. F. Zhang, K. Maslov, G. Stoica, and L. V. Wang, "Three-dimensional imaging of skin melanoma *in vivo* by dual-wavelength photoacoustic microscopy," J. Biomed. Opt. **11**(3), 034032 (2006).
9. L. V. Wang, "Prospects of photoacoustic tomography," Med. Phys. **35**(12), 5758–5767 (2008).
10. S. Hu and L. V. Wang, "Photoacoustic imaging and characterization of the microvasculature," J. Biomed. Opt. **15**(1), 011101 (2010).
11. E. Dimitrow, M. Ziemer, M. J. Koehler, J. Norgauer, K. König, P. Elsner, and M. Kaatz, "Sensitivity and specificity of multiphoton laser tomography for in vivo and ex vivo diagnosis of malignant melanoma," J. Invest. Dermatol. **129**(7), 1752–1758 (2009).
12. D. Fu, T. Ye, T. E. Matthews, G. Yurtsever, and W. S. Warren, "Two-color, two-photon, and excited-state absorption microscopy," J. Biomed. Opt. **12**(5), 054004 (2007).
13. D. Fu, T. Ye, T. E. Matthews, B. J. Chen, G. Yurtserver, and W. S. Warren, "High-resolution in vivo imaging of blood vessels without labeling," Opt. Lett. **32**(18), 2641–2643 (2007).
14. W. Min, S. Lu, S. Chong, R. Roy, G. R. Holtom, and X. S. Xie, "Imaging chromophores with undetectable fluorescence by stimulated emission microscopy," Nature **461**(7267), 1105–1109 (2009).

#147076 - $15.00 USD Received 5 May 2011; revised 13 May 2011; accepted 13 May 2011; pub. 16 May 2011

15. M. Streit and M. Detmar, "Angiogenesis, lymphangiogenesis, and melanoma metastasis," Oncogene **22**(20), 3172–3179 (2003).
16. S. Kizaka-Kondoh, M. Inoue, H. Harada, and M. Hiraoka, "Tumor hypoxia: a target for selective cancer therapy," Cancer Sci. **94**(12), 1021–1028 (2003).
17. G. Zonios, A. Dimou, M. Carrara, and R. Marchesini, "In vivo optical properties of melanocytic skin lesions: common nevi, dysplastic nevi and malignant melanoma," Photochem. Photobiol. **86**(1), 236–240 (2010).
18. H. Hara, N. Walsh, K. Yamada, and K. Jimbow, "High plasma level of a eumelanin precursor, 6-hydroxy-5-methoxyindole-2-carboxylic acid as a prognostic marker for malignant melanoma," J. Invest. Dermatol. **102**(4), 501–505 (1994).
19. S. Takeuchi, W. G. Zhang, K. Wakamatsu, S. Ito, V. J. Hearing, K. H. Kraemer, and D. E. Brash, "Melanin acts as a potent UVB photosensitizer to cause an atypical mode of cell death in murine skin," Proc. Natl. Acad. Sci. U.S.A. **101**(42), 15076–15081 (2004).
20. H. Z. Hill and G. J. Hill, ""UVA, pheomelanin and the carcinogenesis of melanoma," Pigm," Cell Res. **13**, 140–144 (2000).
21. I. R. Piletic, T. E. Matthews, and W. S. Warren, "Probing near-infrared photorelaxation pathways in eumelanins and pheomelanins," J. Phys. Chem. A **114**(43), 11483–11491 (2010).
22. T. E. Matthews, I. R. Piletic, M. A. Selim, M. J. Simpson, and W. S. Warren, "Pump-probe imaging differentiates melanoma from melanocytic nevi," Sci. Transl. Med. **3**(71), 71ra15 (2011).
23. L. P. Cui and W. H. Knox, "Forty-five degree backscattering-mode nonlinear absorption imaging in turbid media," J. Biomed. Opt. **15**(2), 026004 (2010).
24. E. K. Nishimura, S. A. Jordan, H. Oshima, H. Yoshida, M. Osawa, M. Moriyama, I. J. Jackson, Y. Barrandon, Y. Miyachi, and S. Nishikawa, "Dominant role of the niche in melanocyte stem-cell fate determination," Nature **416**(6883), 854–860 (2002).
25. Y. Chudnovsky, A. E. Adams, P. B. Robbins, Q. Lin, and P. A. Khavari, "Use of human tissue to assess the oncogenic activity of melanoma-associated mutations," Nat. Genet. **37**(7), 745–749 (2005).
26. D. Fu, T. E. Matthews, T. Ye, I. R. Piletic, and W. S. Warren, "Label-free *in vivo* optical imaging of microvasculature and oxygenation level," J. Biomed. Opt. **13**(4), 040503 (2008).
27. G. F. Murphy, *Dermatopathology* (W.B. Saunders Company, Philadelphia, 1995).

1. Introduction

Early detection of melanoma is critical to a positive patient outcome, but remains clinically challenging. The current gold standard is excision of the lesion followed by histopathology, but this is not an effective screening method and leads to unnecessary patient trauma and increased medical costs. Optical imaging has had good success in noninvasively studying disease through the use of fluorescence, Raman and absorptive signatures [1–5]. Multiphoton imaging gives microscopic images with cellular resolution and depth selectivity in tissues such as the skin, and is therefore a promising technology for studying and screening melanoma.

Many imaging techniques have been applied to the problem of melanoma. Reflectance confocal microscopy gives good structural images based on reflective and refractive features in skin, such as melanosomes and keratin [6,7]. However, it lacks molecular specificity. Photoacoustic microscopy is a powerful technique with excellent penetration depth for imaging intrinsic absorbers, such as hemoglobin and melanin [8–10]. Vasculature of all size scales and its oxygenation state makes an excellent target for this method, as do any chromophores which can be discriminated based on their linear absorbance. However, chemical varieties of melanin have very similar absorption spectra and therefore cannot be separated by photoacoustic microscopy. Similarly, pigmented lesions can be imaged using the autofluorescence of proteins and melanin, but this has no specific contrast for disease [11].

Two-color pump-probe imaging by modulation transfer is a versatile technique for creating contrast based on a wide range of molecules and nonlinear processes, providing highly specific and functional images of biological and medical samples. Pump-probe imaging has the optical sectioning and scattering resistance properties of multiphoton microscopy but does not rely on the generation of new wavelengths of light, which previously limited the array of possible imaging targets. Contrast can be based on sum-frequency absorption, excited state absorption, ground state depletion or stimulated emission. Fu et al. developed pump-probe imaging of melanin, oxy- and deoxyhemoglobin and acquired *in vivo*

#147076 - $15.00 USD Received 5 May 2011; revised 13 May 2011; accepted 13 May 2011; pub. 16 May 2011

images of microvasculature [12,13], and Min et al. showed *in vivo* imaging based on stimulated emission [14].

Two intrinsic chromophores are relevant to the disease state of melanoma: hemoglobin and melanin. Hemoglobin can be used to track new blood vessel formation and tissue hypoxia, features that both correlate with malignancy [15,16]. Melanin contains information about the location, morphology and biochemical state of melanocytes [17,18]. In human skin, two kinds of melanins are found: eumelanin and pheomelanin. Eumelanin is a brown-black pigment and serves a photoprotective role. Pheomelanin is reddish-yellow, found in higher concentrations in red-haired individuals, and acts as a photosensitizer when exposed to ultraviolet radiation [19,20]. Recently we demonstrated that pump-probe imaging can separate eumelanin and pheomelanin [21]. We investigated excised samples from human pigmented lesions and found eumelanin content was substantially increased in melanoma and that imaging the microscopic distribution of eumelanin and pheomelanin could be used to separate melanomas from benign nevi in a highly sensitive manner [22]. Previously Fu *et al.* performed epi-mode imaging on the surface of densely pigmented humans hairs. Improvements in microscope design and signal collection now allow epi-mode imaging at physiologically relevant depths in scattering tissue. Imaging at depth in tissue a more challenging target because imaging takes place through a turbid medium and we rely on backscattered probe light for detection, which decreases exponentially with depth [23]. We report epi-mode eumelanin / pheomelanin contrast and microvessel imaging in excised human pigmented lesions and noninvasively in animal models for melanoma, extending this technique toward optical biopsy as well as for fundamental research into the growth and evolution of melanoma.

Hybrid xenograft mouse systems were chosen for investigation because they offered the most accurate representation of melanoma in human skin. Mouse genetic models have been fruitful in understanding the genetic mechanisms mediating melanoma pathogenesis. However, there are major structural differences between mouse and human skin tissues, which make it difficult to faithfully and non-invasively perform longitudinal studies on the evolution of melanoma lesions in animal models [24]. To better mimic the tissue environment of human melanomas, we generated a xenograft melanoma model on immunodeficient mice with a mixture of human epidermal cells and human melanoma cells [25]. The regenerated human skin was then monitored by noninvasive pump-probe imaging for melanoma progression.

2. Experimental setup

2.1. Pump-probe imaging by modulation transfer

Pump-probe imaging was carried out in a similar fashion to the method outlined by Fu et al. [26]. A titanium:sapphire mode-locked laser operating at 80 MHz and tuned to 810 nm (Tsunami, Spectra-Physics) synchronously pumped an optical parametric oscillator containing a fan-poled crystal (Mira-OPO, Coherent). The signal wavelength was intracavity doubled to 720 nm, which was modulated at 2 MHz with an acousto-optic modulator for use as the pump beam. The 810 nm beam was left unmodulated for use as the probe beam. A mechanical delay stage allowed control of the interpulse delay, and the two beams were combined on a dichroic mirror and directed into a custom constructed scanning laser microscope. A polarizing beamsplitting cube was placed between the tube lens and the objective, oriented to pass both beams. Light was focused into the sample with a 20X air coupled 0.7 numerical aperture objective (Olympus). Pulse durations were typically ~180 femtoseconds at the sample, as measured by cross-correlation. Probe light backscattered by the sample was collected by the excitation objective in epi-mode. A portion of the backscattered light, which has a randomized polarization, was reflected by a polarizing beamsplitting cube after the objective. Two-photon excited autofluorescence was separated from backscattered probe light with a dichroic mirror and focused onto a photomultiplier tube (Hamamatsu). Probe light was passed through two

#147076 - $15.00 USD Received 5 May 2011; revised 13 May 2011; accepted 13 May 2011; pub. 16 May 2011

dielectric bandpass filters (Chroma) to remove all pump light and focused onto a large area photodiode (PDA55, Thorlabs). A 2.5 MHz low pass filter (Minicircuits) removed high frequency noise from the photodiode. The pump-probe modulation transfer signal was measured by a lock-in amplifier (SR844, Stanford Research Systems) tuned to the modulation frequency. A reference sample of rhodamine 6G was used to set the phase based on a known instantaneous absorptive signal. Images typically were acquired at 13 seconds per frame, limited by the time constant of the lock-in amplifier. Eumelanin / pheomelanin contrast was based on the time delay behavior at each pixel, which was sampled by imaging at 17 separate interpulse delays.

2.2. Ex vivo tissue samples

Human pigmented lesions were excised and imaged fresh, without fixation or treatment. After imaging, lesion type was determined by a dermatopathologist examining H&E stained sections. All human studies were carried out with approval by the institutional review board for clinical investigations.

2.3. Xenograft mouse model

To demonstrate pump-probe imaging *in vivo*, we acquired pump-probe images of a developing melanoma in human skin grafted mice following the method outlined by Chudnovsky et al. [25]. The grafts were prepared as follows: a mixture of primary human keratinocytes and human melanoma cells (A2058) were seeded in a 10:1 ratio onto pieces (around 1 cm^2) of devitalized human dermis, which were kept in culture for 3-4 days until cells reached confluence on and around the dermis. These regenerated skin tissues were xenotransplanted onto *SCID* mice and then imaged with our pump-probe microscope. The graft was implanted on the dorsal skin (back) of the animal. For imaging, mice were anesthetized with isoflurane and mounted on a custom stage of an upright laser scanning microscope. A coverslip was clamped over the dorsal skin graft to immobilize the region, flatten the tissue and minimize motion artifacts. The noninvasive nature of the imaging procedure allowed the grafts to be followed over time. The Institutional Animal Care and Use Committee approved all procedures involving animal research.

3. Results

3.1. Melanin contrast in ex vivo human nevi

We imaged an excised pigmented lesion pumping at 720 nm (15 mW) and probing at 810 nm (15 mW). Melanin in the skin was easily visible and structures as deep as 120 µm could be captured (Fig. 1). Pigmented basal cells along the dermal-epidermal junction and keratinocytes in the superficial layers of the epidermis gave rise to strong signal. Below 20 µm into the tissue, irregular dermal papillae interdigitating with the rete ridges of the epidermis were visualized as a web-like pattern. The papillary dermis contained no melanized cells, and so dermal papillae appeared dark (Fig. 1B, arrowheads). Keratinocytes and melanocytes along the dermal-epidermal junction were heavily pigmented and appeared bright. Pigmented basal cells were found at the base of rete ridges as deep as 120 µm from the surface (Fig. 1F, arrow).

Examination of H&E sections taken from the excised lesion showed it to be a lentigo with hyperpigmentation of the basal layer and elongated rete ridges (Fig. 1G). No nests of melanocytes were found, and the number of melanocytes present in the basal layer was not larger than normal. The epidermis was roughly 20-40 µm in thickness. Rete ridges were elongated to over 100 µm beneath the surface of the skin. No melanocytes or pigmented cells were present in the dermis. Solar damage to the dermis from ultraviolet radiation (solar elastosis) was apparent.

#147076 - $15.00 USD Received 5 May 2011; revised 13 May 2011; accepted 13 May 2011; pub. 16 May 2011

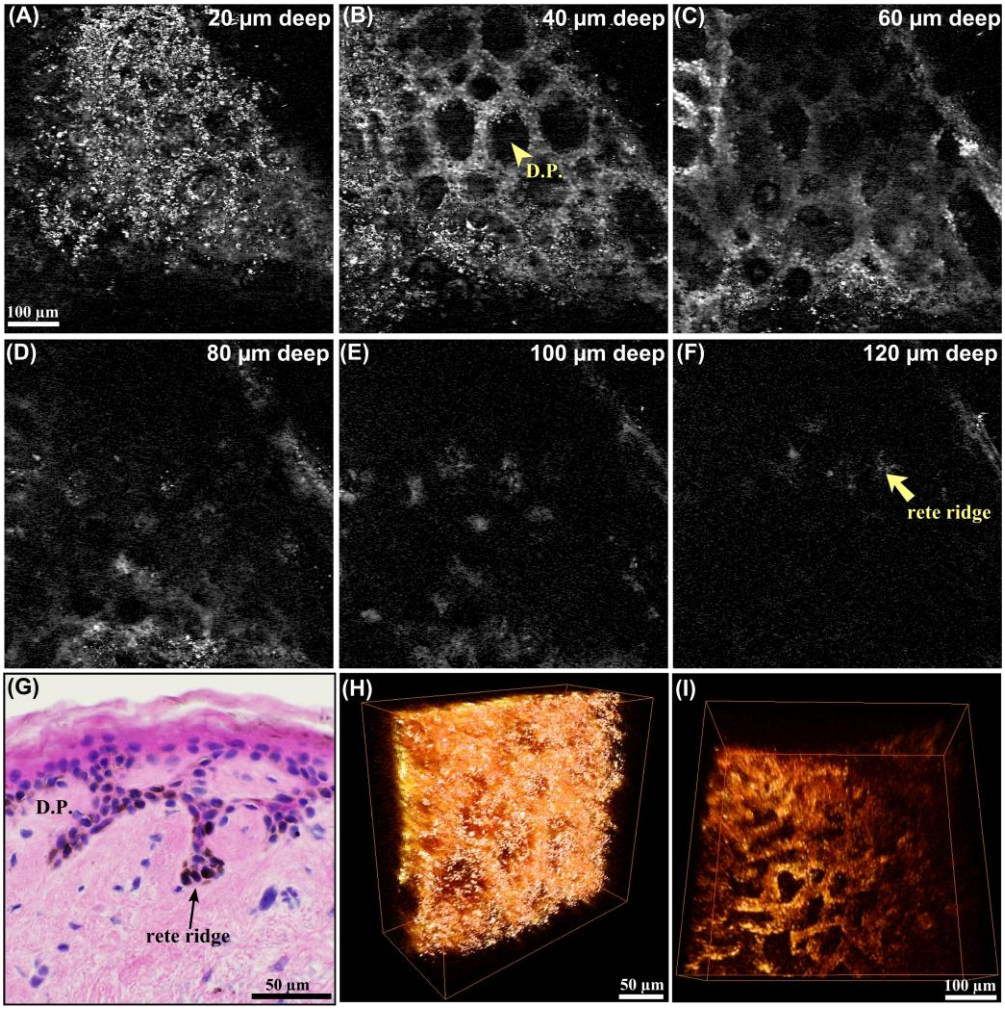

Fig. 1. **(A-F)** Pump-probe epi-mode images of melanin at 0 fs interpulse delay in an excised lesion at 20, 40, 60, 80, 100 and 120 µm below the surface of the skin. At 40 µm deep (**B**), the dermal-epidermal junction was clearly imaged. Epidermal pigmented cells are visible surrounding dermal papillae (arrowhead). Rete ridges 120 µm below the surface (**F**) were observed (arrow). (**G**) H&E stained cross-section from the lesion showing the skin architecture, including dermal papilla (D.P.) and elongated rete ridges extending more than 100 µm below the surface. **(H, I)** 3D reconstructions of various regions from an excised lesion showing local details (Media 1) and a large area with clearly visible rete ridges encompassing the region imaged in Fig. 2. (Media 2).

We were able to differentiate pheomelanin from eumelanin at the dermal-epidermal junction with modest optical power. Pumping with 5 mW and probing with 10 mW, we created maps of the melanin content along the dermal-epidermal junction with cellular detail (Fig. 2). A series of 17 images at different interpulse delays were acquired to sample the transient behavior of melanin. Principal component analysis was used to examine the different delay traces across the image and separate the transient signals of eumelanin from pheomelanin. Eumelanin has been shown to have an excited state absorption signal at these wavelengths, while pheomelanin's transient behavior is described mostly by ground state depletion [21]. Melanin molecular contrast showed the excised lesion to have a generally uniform pigmentation. Most of the observed regions were pheomelanic. However, in one field of view a predominantly eumelanin-containing region was found (Fig. 2A, arrowhead), as

#147076 - $15.00 USD Received 5 May 2011; revised 13 May 2011; accepted 13 May 2011; pub. 16 May 2011

well as regions containing a heterogeneous mix of pigments. Figure 2B shows a region of heterogeneous pigmentation: pheomelanic on average, with some melanocytes expressing eumelanin.

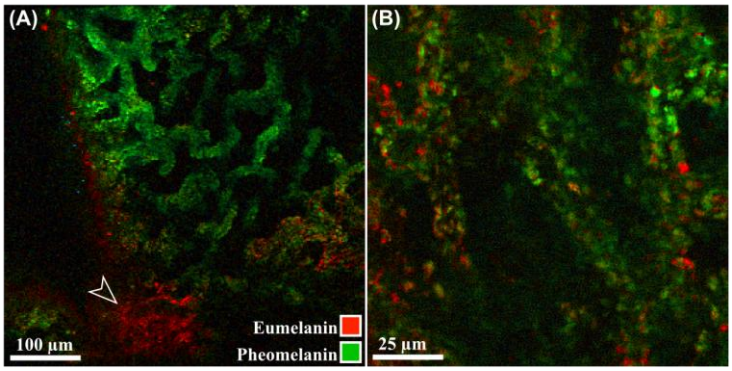

Fig. 2. Melanin principal component epi-mode images showing chemical contrast of an excised lesion. Images were acquired with 5 mW pump power, 10 mW probe power. (**A**) Large field of view acquired 45 µm below the surface showing heavily pigmented rete ridges of relatively uniform composition. Arrowhead denotes a eumelanic region. (**B**) Smaller field of view demonstrating cellular detail acquired 20 µm below the surface. Pigmented keratinocytes are resolved.

3.2. Microvasculature in vivo imaging

Hemoglobin can also be imaged via pump-probe at these wavelengths. Hemoglobin has a purely positive response (due to excited state absorption), while both melanins demonstrate a negative (bleaching) signal at 0 fs interpulse delay. Previously, Fu et al. demonstrated imaging the *in vivo* oxygenation state of microvasculature in transmission mode [26]. Using our adapted setup, we have now imaged microvasculature greater than 100 µm below the surface of the skin in epi-mode (Fig. 3). We examined human skin grafts on our mouse melanoma model 4 weeks after implantation, after vascularization had taken place. Vasculature images were acquired at 0 fs interpulse delay using 19 mW pump power (720 nm) and 40 mW probe power (810 nm). 3D maps of capillaries, venules and arterioles can be simultaneously acquired with melanin images to provide a comprehensive picture of tissue function.

3.3. Melanin molecular contrast in xenograft mice

Figure 4 shows a pump-probe image of our mouse melanoma model containing significant chemical heterogeneity. Two weeks after implantation of the human skin graft, small dark spots appeared (Fig. 4A). Pump-probe imaging found melanin in all layers of the epidermis in one such spot, from the stratum corneum down to the dermal-epidermal junction 50-60 µm below the surface. Melanin was found in relatively pure deposits, with little mixing between eumelanin and pheomelanin. The center of the lesion was very pheomelanic, surrounded by a strongly eumelanic ring. Individual cells appeared to be uniformly pigmented. Fluorescence signals measured by the PMT mostly results from two-photon excited autofluorescence (TPEF) of NADH, elastin and keratin [1]. TPEF is most useful for orienting the melanin deposits and vessels in the skin, as keratin from corneocytes in the stratum corneum gives a very strong signal. This allows for accurate determination of the depth of the field of view, as well as orientation within the skin based on structural changes between the epidermis and dermis.

#147076 - $15.00 USD Received 5 May 2011; revised 13 May 2011; accepted 13 May 2011; pub. 16 May 2011

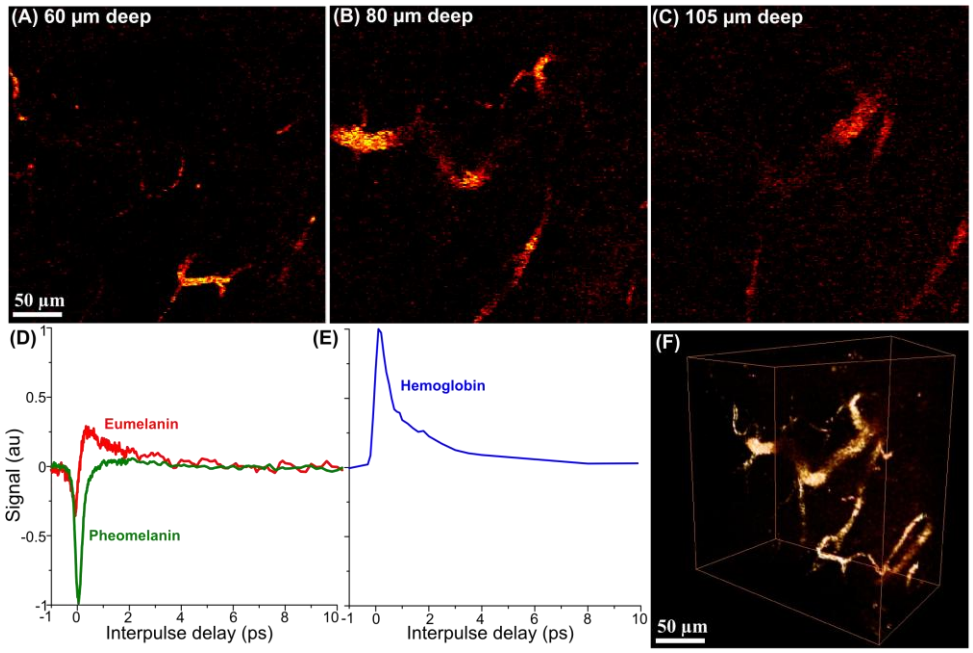

Fig. 3. *In vivo* epi-mode pump-probe images of mouse dermal microvasculature acquired 60, 80, and 105 µm below the surface of the skin at 0 fs interpulse delay **(A, B, C)**. Images were acquired with 19 mW pump and 40 mW probe power. Representative pump-probe delay traces at these wavelengths for eumelanin, pheomelanin and hemoglobin are shown **(D and E)**. Hemoglobin is easily separated by its positive signal at time zero. (**F**) 3D reconstruction of the microvasculature (Media 3).

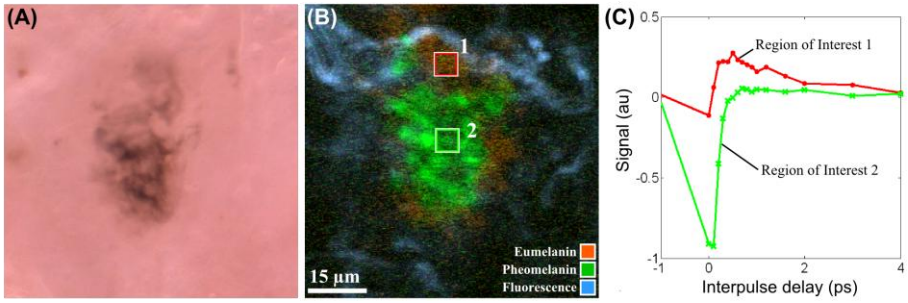

Fig. 4. **(A)** A developing mouse melanoma, brightfield image. (**B**) *In vivo* epi-mode pump-probe images with cellular detail acquired 45 µm below the surface of the skin (25 mW total power) near the basal layer. Principal component images are co-registered with a simultaneously acquired TPEF image (blue). The central region of the tumor was pheomelanic (box 2), surrounded by a ring of eumelanin containing cells (box 1). (**C**) Time delay traces in each region show melanin's characteristic transient behavior.

4. Discussion and conclusion

Important morphological features are captured by pump-probe imaging, including architecture of the epidermis, location and organization of melanocytes and the structure of the local microvasculature. Histopathological markers for melanoma include presence of melanocytes in the epidermis (pagetoid spread), organization of melanocytes into nests, the presence of nests bridging rete ridges, enlarged melanocytes, confluent growth of melanocytes along the dermal-epidermal junction, and the presence of pigmented or immature melanocytes in the dermis [27]. Blood vessel architectural changes are also associated with tumor development: tumors will develop an angiogenic phenotype, producing more blood vessels with an irregular

#147076 - $15.00 USD Received 5 May 2011; revised 13 May 2011; accepted 13 May 2011; pub. 16 May 2011

geometry. Vasculature changes have long been shown for cutaneous melanomas [15]. All of these features can be captured by pump-probe imaging.

More importantly, molecular contrast allows functional mapping of the lesion. We can investigate the behavior of melanocytes by examining the chemical mixture produced by melanogenesis. It has been found that eumelanin content and the chemical heterogeneity of pigmentation allows differentiation between melanoma and benign lesions in biopsy samples. This information can now be acquired *in vivo*. The oxygenation state of blood vessels is relevant to tumor progression as well: Normal tissue will not have regions of severe hypoxia, but many tumors will have chronically and transiently hypoxic regions. Tumor hypoxia correlates with a more malignant phenotype, resistance to treatments, increased metastasis and poor outcomes [16]. By imaging both eumelanin/pheomelanin distributions as well as hemoglobin oxygenation, a full characterization of lesions can be made.

We have demonstrated the viability of noninvasive, epi-mode pump-probe imaging of melanocytic lesions. Pump-probe imaging may also serve as the basis of a powerful diagnostic aid and screening tool for melanoma. Evaluating regions where biopsies are much more difficult to obtain, such as intraocular melanoma, or where tissue conservation is imperative, such as the face, could be very beneficial. This technique opens the door to a more detailed study and richer understanding of the progression of melanoma than has previously been possible.

Acknowledgments

This work was supported by the National Institutes of Health grant 1RC1CA145105 and Duke University. We thank Dr. Angelica Selim for her expert guidance and time spent in discussion evaluating histopathology results.

#147076 - $15.00 USD Received 5 May 2011; revised 13 May 2011; accepted 13 May 2011; pub. 16 May 2011